

The role of surface chemistry and fatigue on tribocorrosion of austenitic stainless steel



A.H. Zavieh^{a,b,*}, N. Espallargas^a

^a NTNU, Norwegian University of Science and Technology, Faculty of Engineering Science and Technology, Department of Engineering Design and Materials, Tribology Lab, N-7491 Trondheim, Norway

^b HSN, Department of Technology, 3616 Kongsberg, Norway

ARTICLE INFO

Article history:

Received 29 April 2016

Received in revised form

24 June 2016

Accepted 24 July 2016

Available online 25 July 2016

Keywords:

Fatigue

Multidegradation

Stainless steel

Surface chemistry

ABSTRACT

Tribocorrosion is combined with fatigue (multi-degradation) in many engineering applications. In the present study, the effect of surface chemistry and electrochemical conditions on multi-degradation of austenitic stainless steel has been investigated. Mechanical and chemical wear loss has been calculated by modeling and measuring anodic current at open circuit potential and passive potential respectively. Surface and subsurface structure and chemistry has been investigated by SEM/FIB and XPS. Observations showed that cyclic and static 4-point bending affect the composition of the passive film and concentration of Mo and Cr cations in the oxide layer as well as formation of subsurface voids and cracks at different electrochemical conditions. Formation $\text{Cr}(\text{OH})_3$ is found to have significant effect on multi-degradation.

© 2016 Elsevier Ltd. All rights reserved.

1. Introduction

Multi-degradation (simultaneous corrosion, wear and fatigue) in marine and offshore industry can result in severe damage and decrease in life span of components and systems used for critical operations [1,2]. Although corrosion, wear and fatigue and their interaction in passive alloys have been subjected to numerous research studies [3–8], only recently multi-degradation phenomena has been studied to some extent [2,9,10].

Many studies were dedicated to understand the factors controlling volume loss in tribocorrosion and multi-degradation in passive alloys and passive films were found to be an important aspect of the phenomena. Bidiville et al. [11] concluded that larger strain accumulation on the near surface in the presence of passive film can result in subsurface cracking and limited plastic flow. Favero et al. [12] showed that the wear accelerated corrosion at passive potentials cannot solely account for increase in wear loss thus, applied potential and formation of passive film should affect mechanical wear loss and therefore the mechanical response of 316L steel is influenced by the presence of passive film and its characteristics. Mischler et al. [13] showed that passivity controls chemical degradation as well as mechanical properties of the surface and it was suggested that depending on the nature of the

electrolyte, plastic deformation is either accompanied by particle detachment or subsurface cracking and delamination.

A lab-scale multi-degradation (LSMD) test rig was developed in 2010 to simulate the offshore environment and operation conditions [9]. The LSMD test rig can reproduce the simultaneous effect of wear, corrosion and 4-point bending action on a desired system. Studying multi-degradation, von der Ohe et al. [10] showed the effect of electrochemical conditions on wear loss. It was suggested by the authors that the oxide film plays a significant role in multi-degradation mechanisms however this role has not been studied in depth and effect of surface chemistry and passive film compounds on multi-degradation remained unclear [10].

Other studies focused on the chemical composition and mechanical properties of passive films. A. Alamr [14] and R.S. Yassar [15] have studied the effect of surface chemistry on the nano-indentation fracture load of the passive film formed on different stainless steels under different growing conditions. It was found that the fracture loads are directly related to the crystallography of the passive films and the Fe and Cr content at the surface. Decreasing the ratio of iron to other metallic elements in the passive film leads to an increase in the load required to fracture the film. It was also suggested that the $\text{Cr}^{6+}/\text{Cr}^{3+}$ ratio affect the film strength and the degree of crystallinity of the passive film. When this ratio is high the crystallinity of the passive film decreases and the fracture load of the passive film are lower. Moreover Clayton [16] showed that formation of $\text{Cr}(\text{OH})_3$ inclusions in the passive film promotes localized corrosion thus more material loss. Willenbruch et al. [17] proposed that Mo influences the formation of

* Corresponding author at: NTNU, Norwegian University of Science and Technology, Faculty of Engineering Science and Technology, Department of Engineering Design and Materials, Tribology Lab, N-7491 Trondheim, Norway.

E-mail address: amin.h.zavieh@ntnu.no (A.H. Zavieh).

more stable intermetallic compounds of Cr^{6+} and Cr^{3+} on the surface thus increasing the stability of the passive film. Montemor et al. [18] suggested that Mo compounds retard the corrosion process by adsorption of corrosive species (e.g. Cl^- and H_3O^+) and the presence of Mo^{6+} thickens the passive film as more stable Cr compounds are formed.

In our previous work, the effect of chemical composition of the alloy on the characteristics of the passive film and its significant role on the multi-degradation of austenitic and duplex stainless steels was studied [19]. However the role of the chemistry of the passive film on multi-degradation at different bending conditions is still little understood. This paper aims to further investigate the role of surface chemistry and passive film characteristics of austenitic stainless steel exposed to tribocorrosion-fatigue (multi-degradation) at different electrochemical and mechanical conditions. The main focus of this study will be on better understanding of the formation of different surface oxides and their role in mechanical and chemical losses in multi-degradation.

2. Experimental procedure

2.1. Material

Austenitic stainless steel UNS S31603 (ASS) was chosen as the test material. The chemical composition and tensile stress ($\text{Rp}_{0.2}$) of the alloy according to material certificates is shown in Table 1. Test samples were cut and machined in the size of 400 mm × 30 mm × 10 mm. Specimens surfaces were grinded to 1000 grit SiC paper and then cleaned in ultrasonic ethanol and distilled water baths prior to experiment. They were coated with two component epoxy paint (Jotamastic 90, Jotun) and covered with polyolefin heat-shrinkable tubes on the contact points with the supports to avoid any damage to the coating during cyclic bending. The area of 15 cm² on the samples was left uncoated to be in contact with Alumina reciprocating ball and exposed to 3.4 wt% NaCl electrolyte to simulate seawater and performing electrochemical measurements. More details on sample geometry and preparation can be found elsewhere [9].

2.2. Multi-degradation tests and electrochemical measurements

Polarization curves of the material were recorded in the electrolyte after stabilization for 10 min at a scan rate of 5 mV/min (one repetition is shown in Fig. 1). The polarization curves were used to distinguish cathodic and anodic regions to perform potentiostatic multi-degradation tests under cathodic and passive potentials.

Multi-degradation (tribocorrosion-fatigue and tribocorrosion) tests were performed using a lab-scale multi-degradation (LSMD) test rig [9]. The LSMD test rig consists of 6 test chambers each provides 4-point static or cyclic (fatigue) bend testing while applying reciprocating rubbing on the tensile loaded side of the exposed test surface in desired electrolyte, in addition it includes arrangements for performing electrochemical measurements.

The reciprocating sliding motion was performed using polished

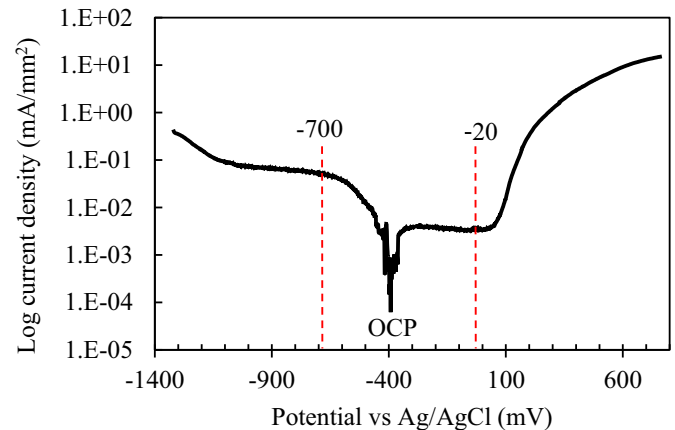


Fig. 1. Polarization curve of ASS in 3.4 wt.% NaCl at a scan rate of 5 mV/min.

alumina ball (Al_2O_3 , \varnothing 4.76 mm) cleaned in ultrasonic ethanol and distilled water baths prior to experiments. The electrolyte chosen was 3.4 wt% NaCl solution at room temperature. All tribocorrosion tests were performed at 6000 reciprocating cycles at a sliding frequency of 1 Hz with a stroke length of 20 mm regardless the testing condition. The tests were performed at five different conditions: (1) without bending (i.e. tribocorrosion), (2–4) Cyclic bending (i.e. tribocorrosion-fatigue) with bending frequencies of 0.25, 1.25 and 2.25 Hz equal to 90% of $\text{Rp}_{0.2}$ and (5) Static bending at 90% of $\text{Rp}_{0.2}$. For clarity and simplicity, in the rest of the manuscript the different testing conditions will be simply referred to as (1) “no bending”, (2–4) “X.XX Hz bending” and (5) “static bending”.

Each set of experiment was performed at cathodic -700 mV vs Ag/AgCl reference, open circuit potential (OCP) as well as passive potential -20 mV. In all sets of experiments, samples were held at OCP for 10 min before and after testing to stabilize the electrochemical cell. All tests were performed at least 2 times for repeatability purposes. Moreover, coefficient of friction (COF), bending stress and temperature, were recorded during the experiments. The full test matrix can be found in Table 2. Potential versus Ag/AgCl 3 M KCl reference electrode was measured by ACM instrument field machine potentiostat.

2.3. Characterization of the materials after testing

Alicona InfiniteFocus 3D optical microscope was used for the determination of wear volume. Quantification of the volume of the wear scars was done by setting the surface of the specimen 3 mm away from the wear track as the reference surface, average depth and width was measured then a triangle was assumed as the cross-section of the wear track. Microhardness measurements were performed by Mitutoyo HM-200 series micro Vickers hardness testing machine 100 gf was chosen as load with the duration of 15 s loading.

FEI Helios NanoLab DualBeam focused ion beam (FIB) was used for scanning electron microscopy (SEM) and cross-section preparation. Deposition, milling and polishing was performed by gallium liquid metal ion source. Cross beam microscopy with Everhart-Thornley detector revealed the wear track morphology and grain contrast. Milling performed after deposition of a 2 μm thick protective carbon layer on the surface to avoid formation of artifacts such as curtains. This layer can be seen as a black layer on the surface in FIB images. A trench with depth of 18 μm was milled with high current (20 nA, 30 kV), then the cross-section was finally cleaned using lower currents (from 6.5 nA to 90 pA) to get maximum grain contrast which is observed due to electron channeling effect.

Table 1
Chemical composition and properties of test samples.

Metal alloy	Sample acronym	Chemical composition (wt%)	$\text{Rp}_{0.2}$ (MPa)
UNS S31603	ASS	0.019 C, 0.92 Mn, 0.022 P, 0.004 S, 0.46 Si, 16.79 Cr, 10.12 Ni, 2.08 Mo, 0.01 N,	333

Download English Version:

<https://daneshyari.com/en/article/614061>

Download Persian Version:

<https://daneshyari.com/article/614061>

[Daneshyari.com](https://daneshyari.com)